

Three WASP-South transiting exoplanets: WASP-74b, WASP-83b & WASP-89b

Coel Hellier¹, D.R. Anderson¹, A. Collier Cameron², L. Delrez³, M. Gillon³, E. Jehin³, M. Lendl^{3,4}, P.F.L. Maxted¹, F. Pepe⁴, D. Pollacco⁵, D. Queloz^{4,6}, D. Ségransan⁴, B. Smalley¹, A.M.S. Smith^{1,7}, J. Southworth¹, A.H.M.J. Triaud^{4,8}, O.D. Turner¹, S. Udry⁴,
& R.G. West⁵

ABSTRACT

We report the discovery of three new transiting hot Jupiters by WASP-South together with the TRAPPIST photometer and the Euler/CORALIE spectrograph.

WASP-74b orbits a star of $V = 9.7$, making it one of the brighter systems accessible to Southern telescopes. It is a $0.95 M_{\text{Jup}}$ planet with a moderately bloated radius of $1.5 R_{\text{Jup}}$ in a 2-d orbit around a slightly evolved F9 star.

WASP-83b is a Saturn-mass planet at $0.3 M_{\text{Jup}}$ with a radius of $1.0 R_{\text{Jup}}$. It is in a 5-d orbit around a fainter ($V = 12.9$) G8 star.

WASP-89b is a $6 M_{\text{Jup}}$ planet in a 3-d orbit with an eccentricity of $e = 0.2$. It is thus similar to massive, eccentric planets such as XO-3b and HAT-P-2b, except that those planets orbit F stars whereas WASP-89 is a K star. The $V = 13.1$ host star is magnetically active, showing a rotation period of 20.2 d, while star spots are visible in the transits. There are indications that the planet's orbit is aligned with the stellar spin. WASP-89 is a good target for an extensive study of transits of star spots.

Subject headings: planetary systems — stars: individual (WASP-74, WASP-83, WASP-89)

1. Introduction

The combination of the WASP-South survey instrument, the Euler/CORALIE spectrograph and

the robotic TRAPPIST photometer continue to be an efficient team for the discovery of transiting exoplanets around stars of $V = 9\text{--}13$ in the Southern Hemisphere (e.g. Hellier et al. 2014; Anderson et al. 2014a). Ongoing discoveries are important for expanding our census of the hot-Jupiter population, while exoplanets transiting relatively bright stars are good targets for followup studies. In this paper we report three new discoveries: WASP-74b, which orbits a bright $V = 9.7$ star; WASP-83b, a more moderately bloated Saturn-mass planet, which, with a period of 4.97 d demonstrates the capability of a single-longitude transit search to find planets with integer-day periods; and WASP-89b, a massive planet in a short and eccentric orbit around a magnetically active K star.

¹Astrophysics Group, Keele University, Staffordshire, ST5 5BG, UK

²SUPA, School of Physics and Astronomy, University of St. Andrews, North Haugh, Fife, KY16 9SS, UK

³Institut d'Astrophysique et de Géophysique, Université, Liège, Allée du 6 Août, 17, Bat. B5C, Liège 1, Belgium

⁴Observatoire astronomique de l'Université de Genève, 51 ch. des Maillettes, 1290 Sauverny, Switzerland

⁵Department of Physics, University of Warwick, Gibbet Hill Road, Coventry CV4 7AL, UK

⁶Cavendish Laboratory, J J Thomson Avenue, Cambridge, CB3 0HE, UK

⁷N. Copernicus Astronomical Centre, Polish Academy of Sciences, Bartycka 18, 00-716 Warsaw, Poland

⁸Department of Physics and Kavli Institute for Astrophysics & Space Research, Massachusetts Institute of Technology, Cambridge, MA 02139, USA

2. Observations

The observational and analysis techniques used here are similar to those in recent WASP-South discovery papers (e.g. Hellier et al. 2012; Anderson et al. 2014b), and so are reported briefly. WASP-South surveys the Southern sky using an array of 200mm f/1.8 lenses and a cadence of ~ 10 mins (see Pollacco et al. 2006). Transit searching of accumulated lightcurves (Collier-Cameron et al. 2007a) leads to tens of thousands of possible candidates, of which the vast majority are false alarms resulting from the limitations of the photometry. The best 1 per cent are selected by eye as candidates and are passed to TRAPPIST (a robotic 0.6-m photometric telescope) and to the 1.2-m Euler/CORALIE spectrograph (for radial-velocity observations). About 1 in 12 candidates turns out to be a planet, with most of the others being astrophysical transit mimics (blended or grazing eclipsing binaries). Higher-quality transit lightcurves are then obtained with TRAPPIST (Jehin et al. 2011) and with EulerCAM (Lendl et al. 2012). We have also observed a transit of WASP-74b using RISE on the Liverpool Telescope (see Steele et al. 2008).

A list of the observations reported here is given in Table 1 while the CORALIE radial velocities are listed in Table A1.

3. The host stars

We used the CORALIE spectra to analyse the three host stars, co-adding the standard pipeline reduction products to produce spectra with S/N ratios of 150:1, 100:1 and 30:1 for WASP-74, WASP-83 and WASP-89 respectively. Our analysis methods are described in Doyle et al. (2013). The effective temperature (T_{eff}) estimate comes from the excitation balance of Fe I lines, while the surface gravity ($\log g$) estimates comes from the ionisation balance of Fe I and Fe II and the Ca I line at 6439Å and the Na I D lines. The metallicity was determined from equivalent width measurements of several unblended lines. The quoted error estimates include that given by the uncertainties in T_{eff} and $\log g$, as well as the scatter due to measurement and atomic data uncertainties.

The projected stellar rotation velocity ($v \sin i$) was determined by fitting the profiles of several unblended Fe I lines. Values of macroturbulent

Table 1: Observations

Facility	Date	
WASP-74:		
WASP-South	2010 May–2012 Jun	10 000 points
CORALIE	2011 Aug–2012 Oct	20 RVs
EulerCAM	2012 May 07	Gunn r filter
TRAPPIST	2012 May 07	z' band
EulerCAM	2012 May 22	Gunn r filter
TRAPPIST	2012 May 22	z' band
TRAPPIST	2012 Jun 21	z' band
TRAPPIST	2012 Jun 23	z' band
TRAPPIST	2012 Sep 04	z' band
TRAPPIST	2013 Jun 27	$I + z$ band
LT/RISE	2014 Aug 19	$V + R$
WASP-83:		
WASP-South	2006 May–2010 Jun	20 600 points
CORALIE	2011 Mar–2013 Feb	28 RVs
TRAPPIST	2012 Jan 07	Blue-block filter
TRAPPIST	2012 Jan 22	Blue-block filter
TRAPPIST	2012 Feb 06	Blue-block filter
WASP-89:		
WASP-South	2008 Jun–2012 Jun	18 000 points
CORALIE	2011 May–2013 May	20 RVs
TRAPPIST	2012 Aug 26	Blue-block filter
EulerCAM	2012 Sep 12	Gunn r filter
TRAPPIST	2012 Sep 12	Blue-block filter
EulerCAM	2012 Oct 02	Gunn r filter
TRAPPIST	2012 Oct 02	Blue-block filter
TRAPPIST	2013 Jun 14	Blue-block filter
TRAPPIST	2013 Aug 27	Blue-block filter

velocity of $3.9 \pm 0.7 \text{ km s}^{-1}$ and $2.9 \pm 0.7 \text{ km s}^{-1}$ were adopted for WASP-74 and WASP-83, using the calibration of Doyle et al. (2014). For WASP-89, however, macroturbulence was assumed to be zero, since for mid-K stars it is expected to be lower than that of thermal broadening (Gray 2008).

The parameters obtained from the analysis are given in Tables 2 to 4. The quoted spectral type derives from T_{eff} , using the values in Gray (2008). Abundances are relative to the solar values obtained by Asplund et al. (2009). Gyrochronological age estimates derive from the measured $v \sin i$, assuming that the star's spin is perpendicular to us, so that this is the true equatorial speed. This is then combined with the stellar radius to give a rotational period, to compare with the values

in Barnes (2007). Lithium age estimates come from values in Sestito & Randich (2005). We also list proper motions from the UCAC4 catalogue of Zacharias et al. (2013).

We searched the WASP photometry of each star for rotational modulations by using a sine-wave fitting algorithm as described by Maxted et al. (2011). We estimated the significance of periodicities by subtracting the fitted transit lightcurve and then repeatedly and randomly permuting the nights of observation. We found a significant modulation in WASP-89 (see Section 8.1) but not in the other two stars.

4. System parameters

The CORALIE radial-velocity measurements were combined with the WASP, EulerCAM and TRAPPIST photometry in a simultaneous Markov-chain Monte-Carlo (MCMC) analysis to find the system parameters. For details of our methods see Collier Cameron et al. (2007b). The limb-darkening parameters are noted in each Table, and are taken from the 4-parameter non-linear law of Claret (2000).

For WASP-89b the orbital eccentricity is significant and was fitted as a free parameter. For WASP-74b and WASP-83b we imposed a circular orbit during the analysis (see Anderson et al. 2012 for the rationale for this).

The fitted parameters were T_c , P , ΔF , T_{14} , b , K_1 , where T_c is the epoch of mid-transit, P is the orbital period, ΔF is the fractional flux-deficit that would be observed during transit in the absence of limb-darkening, T_{14} is the total transit duration (from first to fourth contact), b is the impact parameter of the planet's path across the stellar disc, and K_1 is the stellar reflex velocity semi-amplitude. The transit lightcurves lead directly to stellar density but one additional constraint is required to obtain stellar masses and radii, and hence full parametrisation of the system. Here we use the calibrations presented by Southworth (2011), based on masses, radii and effective temperatures of eclipsing binaries.

For each system we list the resulting parameters in Tables 2 to 4, and plot the resulting data and models in Figures 1 to 4. We also refer the reader to Smith et al. (2012) who present an extensive analysis of the effect of red noise in the transit

Table 2: System parameters for WASP-74.
 1SWASP J201809.32–010432.6
 2MASS 20180931–0104324
 RA = $20^{\text{h}}18^{\text{m}}09.32^{\text{s}}$, Dec = $-01^{\circ}04'32.6''$ (J2000)
 V mag = 9.7
 Rotational modulation < 0.7 mmag (95%)
 pm (RA) 1.6 ± 1.0 (Dec) -64.3 ± 0.7 mas/yr

Stellar parameters from spectroscopic analysis.	
Spectral type	F9
T_{eff} (K)	5990 ± 110
$\log g$	4.39 ± 0.07
$v \sin I$ (km s^{-1})	4.1 ± 0.8
[Fe/H]	$+0.39 \pm 0.13$
$\log A(\text{Li})$	2.74 ± 0.09
Age (Lithium) [Gy]	$0.5 \sim 2$
Age (Gyro) [Gy]	$2.0^{+1.6}_{-1.0}$
Distance [pc]	120 ± 20
Parameters from MCMC analysis.	
P (d)	2.137750 ± 0.000001
T_c (HJD) (UTC)	$245\,6506.8918 \pm 0.0002$
T_{14} (d)	0.0955 ± 0.0008
$T_{12} = T_{34}$ (d)	0.0288 ± 0.0014
$\Delta F = R_P^2/R_*^2$	0.00961 ± 0.00014
b	0.860 ± 0.006
i ($^{\circ}$)	79.81 ± 0.24
K_1 (km s^{-1})	0.1141 ± 0.0014
γ (km s^{-1})	-15.767 ± 0.001
e	0 (adopted) (< 0.07 at 3σ)
M_* (M_{\odot})	1.48 ± 0.12
R_* (R_{\odot})	1.64 ± 0.05
$\log g_*$ (cgs)	4.180 ± 0.018
ρ_* (ρ_{\odot})	0.338 ± 0.018
T_{eff} (K)	5970 ± 110
M_P (M_{Jup})	0.95 ± 0.06
R_P (R_{Jup})	1.56 ± 0.06
$\log g_P$ (cgs)	2.95 ± 0.02
ρ_P (ρ_J)	0.25 ± 0.02
a (AU)	0.037 ± 0.001
$T_{P,A=0}$ (K)	1910 ± 40
Errors are 1σ ; Limb-darkening coefficients were: Trap z: $a_1 = 0.757$, $a_2 = -0.591$, $a_3 = 0.890$, $a_4 = -0.416$ Euler & RISE: $a_1 = 0.669$, $a_2 = -0.284$, $a_3 = 0.765$, $a_4 = -0.395$	

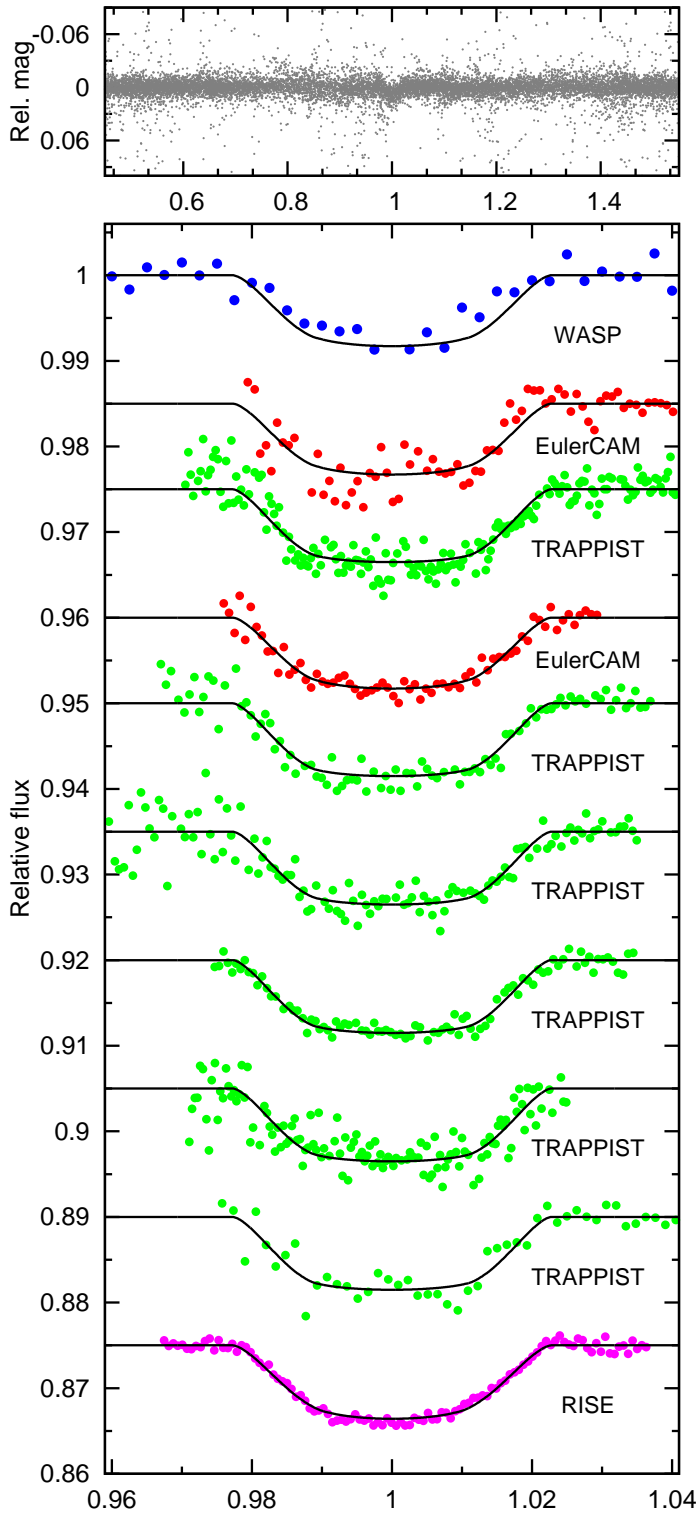


Fig. 1.— WASP-74b discovery photometry: (Top) The WASP data folded on the transit period. (Second panel) The binned WASP data with (offset) the follow-up transit lightcurves (ordered from the top as in Table 1) together with the fitted MCMC model. The two EulerCAM lightcurves are of the same transit as the TRAPPIST data

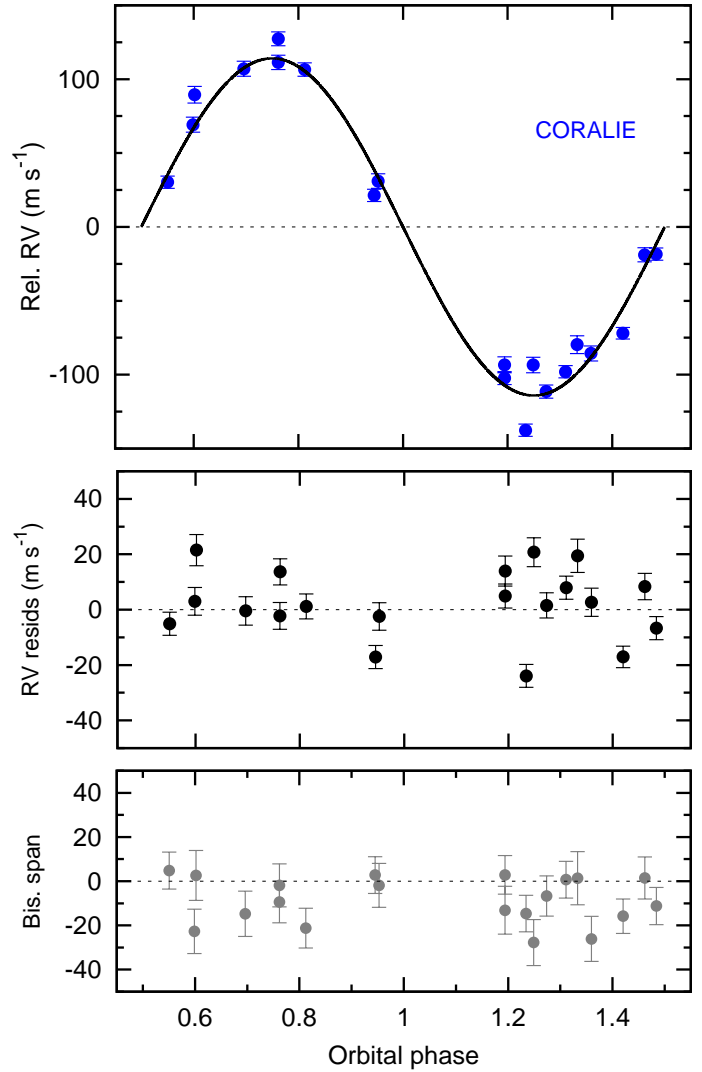


Fig. 2.— WASP-74b radial velocities and fitted model (top) along with (middle) the residuals and (bottom) the bisector spans; the absence of any correlation with radial velocity is a check against transit mimics.

Table 3: System parameters for WASP-83.
 1SWASP J124036.51–191703.4
 2MASS 12403650–1917032
 RA = 12^h40^m36.51^s, Dec = –19°17′03.4″ (J2000)
 V mag = 12.9
 Rotational modulation < 1.5 mmag (95%)
 pm (RA) –21.6 ± 1.9 (Dec) –11.5 ± 2.1 mas/yr

Stellar parameters from spectroscopic analysis.	
Spectral type	G8
T_{eff} (K)	5480 ± 110
log g	4.34 ± 0.08
$v \sin I$ (km s ^{–1})	< 0.5
[Fe/H]	+0.29 ± 0.12
log A(Li)	< 0.75
Age (Lithium) [Gy]	≥ 5
Distance [pc]	300 ± 50
Parameters from MCMC analysis.	
P (d)	4.971252 ± 0.000015
T_c (HJD) (UTC)	245 5928.8853 ± 0.0004
T_{14} (d)	0.1402 ± 0.0015
$T_{12} = T_{34}$ (d)	0.0136 ± 0.0017
$\Delta F = R_p^2/R_*^2$	0.0104 ± 0.0004
b	0.23 ± 0.15
i (°)	88.9 ± 0.7
K_1 (km s ^{–1})	0.0329 ± 0.0031
γ (km s ^{–1})	31.549 ± 0.002
e	0 (adopted) (< 0.3 at 3 σ)
M_* (M_\odot)	1.11 ± 0.09
R_* (R_\odot)	1.05 ^{+0.06} _{–0.04}
log g_* (cgs)	4.44 ^{+0.02} _{–0.04}
ρ_* (ρ_\odot)	0.97 ^{+0.07} _{–0.13}
T_{eff} (K)	5510 ± 110
M_P (M_{Jup})	0.30 ± 0.03
R_P (R_{Jup})	1.04 ^{+0.08} _{–0.05}
log g_P (cgs)	2.79 ± 0.06
ρ_P (ρ_J)	0.26 ± 0.05
a (AU)	0.059 ± 0.001
$T_{P,A=0}$ (K)	1120 ± 30

Errors are 1 σ ; Limb-darkening coefficients were:
 a1 = 0.747, a2 = –0.649, a3 = 1.277, a4 = –0.584

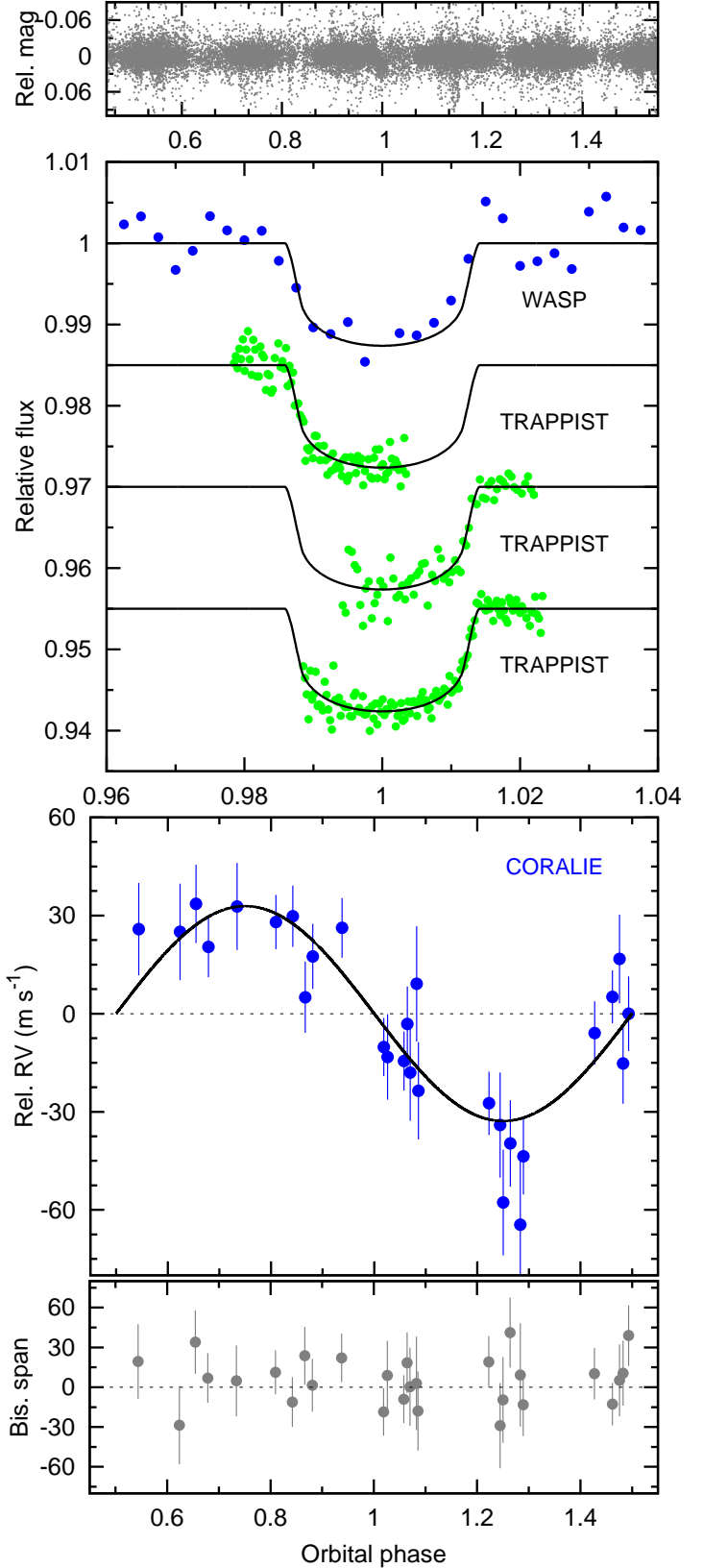


Fig. 3.— WASP-83b discovery data, as for Figs. 1 and 2.

Table 4: System parameters for WASP-89.
 1SWASP J205535.98–185816.1
 2MASS 20553599–1858159
 RA = 20^h55^m35.98^s, Dec = –18°58′16.1″ (J2000)
 V mag = 13.1
 pm (RA) 13.7 ± 1.5 (Dec) –63.0 ± 1.4 mas/yr

Stellar parameters from spectroscopic analysis.

Spectral type	K3
T_{eff} (K)	4955 ± 100
log g	4.31 ± 0.16
$v \sin I$ (km s ^{–1})	2.5 ± 0.9
[Fe/H]	+0.15 ± 0.14
log A(Li)	< 0.24
Age (Lithium) [Gy]	≥ 0.5
Age (Gyro) [Gy]	1.3 ^{+1.5} _{–0.8}

Parameters from MCMC analysis.

P (d)	3.3564227 ± 0.0000025
T_c (HJD) (UTC)	245 6207.02114 ± 0.00012
T_{14} (d)	0.1025 ± 0.0004
$T_{12} = T_{34}$ (d)	0.0112 ± 0.0003
$\Delta F = R_p^2/R_*^2$	0.0149 ± 0.0002
b	0.10 ± 0.08
i (°)	89.4 ± 0.5
K_1 (km s ^{–1})	0.848 ± 0.013
γ (km s ^{–1})	21.088 ± 0.008
e	0.193 ± 0.009
ω (deg)	28 ± 4
M_* (M_\odot)	0.92 ± 0.08
R_* (R_\odot)	0.88 ± 0.03
log g_* (cgs)	4.515 ± 0.018
ρ_* (ρ_\odot)	1.36 ± 0.07
T_{eff} (K)	5130 ± 90
M_p (M_{Jup})	5.9 ± 0.4
R_p (R_{Jup})	1.04 ± 0.04
log g_p (cgs)	4.10 ± 0.02
ρ_p (ρ_J)	5.27 ± 0.33
a (AU)	0.0427 ± 0.0012
$T_{p,A=0}$ (K)	1120 ± 20

Errors are 1 σ ; Limb-darkening coefficients were:
 a1 = 0.741, a2 = –0.739, a3 = 1.427, a4 = –0.620

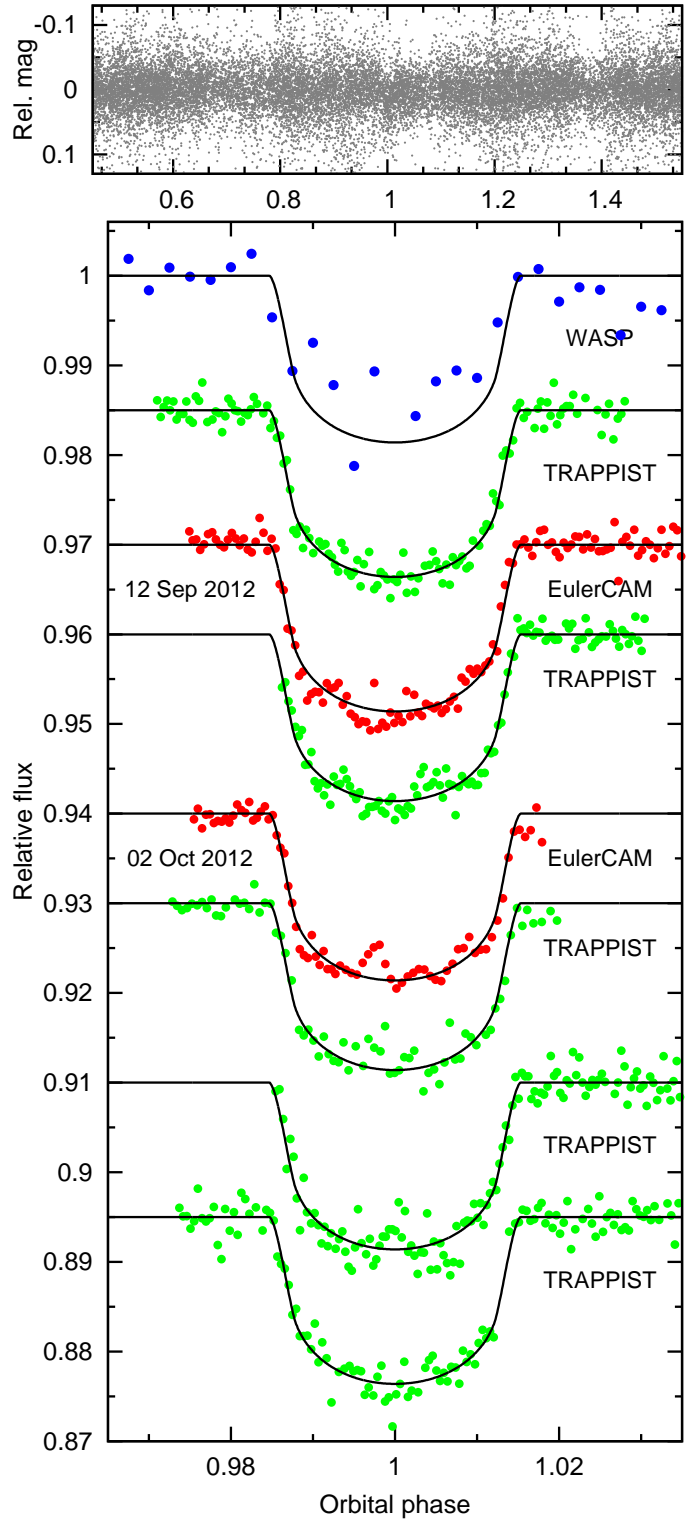


Fig. 4.— WASP-89b discovery data. The Euler and TRAPPIST observations on 12 Sep 2012 and on 02 Oct 2012 are of the same transit, and hence these transits are plotted slightly closer together. Otherwise the lightcurves are as for Fig. 1

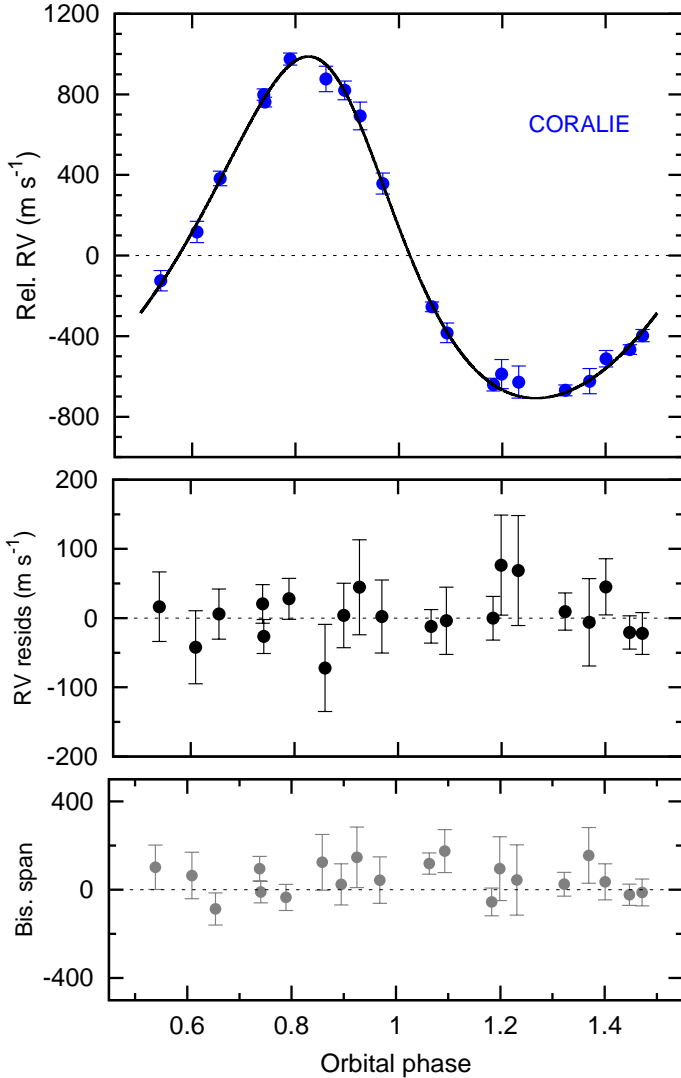


Fig. 5.— WASP-89b radial velocities (as for Fig. 2).

lightcurves on the resulting system parameters.

5. Evolutionary status

One area where the methods of this paper differ from those of previous WASP-South discoveries is in the comparison of the stellar parameters to evolutionary models. Here we use the method described in Maxted, Serenelli & Southworth (2014). This uses an MCMC method to calculate the posterior distribution for the mass and age estimates of the star, by comparing the observed values of ρ_* , T_{eff} and $[\text{Fe}/\text{H}]$ to a grid of stellar models. The stellar models were calculated using the GARSTEC stellar evolution code (Weiss & Schlattl (2008) and the methods used to calculate the stellar model grid are described in Serenelli et al. (2013). The results of this Bayesian analysis are given in Table 5 and are shown in Fig. 6.

6. WASP-74

WASP-74 is a $V = 9.7$, F9 star with a metallicity of $[\text{Fe}/\text{H}] = +0.39 \pm 0.13$. The transit analysis gives a mass and radius of $1.48 \pm 0.12 M_{\odot}$ and $1.64 \pm 0.05 R_{\odot}$. The transit $\log g_*$ of 4.20 ± 0.02 compares to a spectroscopic $\log g_*$ of 4.39 ± 0.07 . The evolutionary comparison (Fig. 6) suggests an evolved star with an age of 3.7 ± 0.9 Gyr and a lower mass of $1.31 \pm 0.06 M_{\odot}$. The gyrochronological and lithium age estimates are lower at $2.0^{+1.6}_{-1.0}$ Gyr and $\gtrsim 2$ Gyr respectively.

The planet, WASP-74b, is a relatively typical hot Jupiter in a 2-d orbit, having a mass of $0.95 \pm 0.06 M_{\text{Jup}}$ and a moderately bloated radius of

Table 5: Bayesian mass and age estimates for the host stars. Columns 2 and 3 give the maximum-likelihood estimates of the age and mass, respectively. Columns 4 and 5 give the mean and standard deviation of the posterior age and mass distribution, respectively.

Star	τ_b [Gyr]	M_b [M_{\odot}]	$\langle \tau_* \rangle$ [Gyr]	$\langle M_* \rangle$ [M_{\odot}]
WASP-74	3.5	1.32	3.7 ± 0.9	1.31 ± 0.06
WASP-83	6.3	1.01	7.1 ± 2.9	1.00 ± 0.05
WASP-89	14.9	0.81	12.5 ± 3.1	0.84 ± 0.04
WASP-89 ^a	1.8	0.91	5.1 ± 3.3	0.87 ± 0.04

^a Assuming $\alpha_{\text{MLT}} = 1.22$

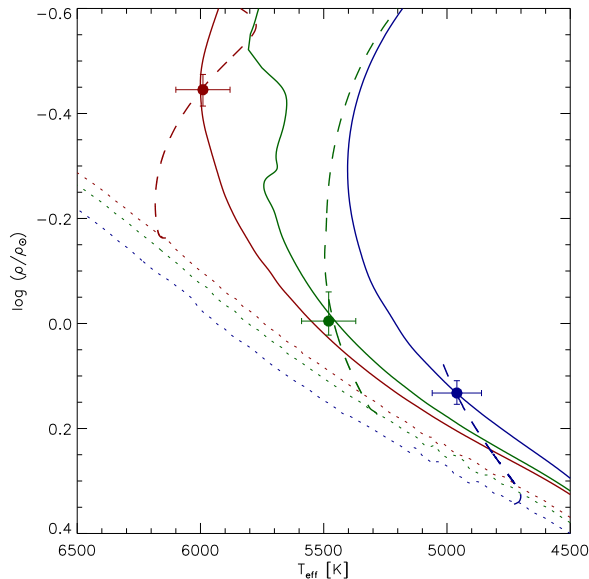


Fig. 6.— Mean stellar density versus effective temperature for WASP-74 (red), WASP-83 (green) and WASP-89 (blue). The best-fit isochrones (color-coded solid lines) are at 3.7 Gyr (WASP-74), 7.1 Gyr (WASP-83) and 5.1 Gyr (WASP-89). The stellar evolution tracks (color-coded dashed lines) are for masses $1.31 M_{\odot}$ (WASP-74), $1.00 M_{\odot}$ (WASP-83) and $0.87 M_{\odot}$ (WASP-89). Lines for each star were interpolated from our grid of GARSTEC models with $\alpha_{\text{MLT}} = 1.78$ using the parameters given in Table 5 and the appropriate value of $[\text{Fe}/\text{H}]$ for each star. The dotted line shows an isochrone at an age of 0.1 Gyr at the same values of $[\text{Fe}/\text{H}]$.

$1.56 \pm 0.06 R_{\text{Jup}}$.

7. WASP-83

WASP-83 is a fainter G8 star of $V = 12.9$, with a metallicity of $[\text{Fe}/\text{H}] = +0.29 \pm 0.12$. The spectroscopic $\log g$ of 4.34 ± 0.08 is compatible with the transit $\log g$ of $4.44^{+0.02}_{-0.04}$. The mass of $1.11 \pm 0.06 M_{\odot}$ from the transit analysis is in line with the evolutionary estimate of $1.00 \pm 0.05 M_{\odot}$. The evolutionary age of 7.1 ± 2.9 Gyr is in line with the lithium age of $\gtrsim 5$ Gyr while the $v \sin i$ of $< 0.5 \text{ km s}^{-1}$ also implies an old star.

The planet, WASP-83b, has a mass of $0.30 \pm 0.03 M_{\text{Jup}}$, matching that of Saturn, and a moderately bloated radius of $1.04^{+0.08}_{-0.04} R_{\text{Jup}}$. It is very similar to WASP-21b (Bouchy et al. 2010), which has a similar mass ($0.3 M_{\text{Jup}}$), is also bloated ($1.2 R_{\text{Jup}}$), and also has a 4-d orbit around a G star.

8. WASP-89

With a magnitude of $V = 13.1$, WASP-89 is among the faintest planet-hosts found by WASP-South, but is among the more interesting systems. The spectroscopy (with a low S/N owing to the faintness) reports it as a K3 star with $\log g = 4.31 \pm 0.16$ and a mass of $0.88 \pm 0.08 M_{\odot}$. The transit analysis gives $\log g = 4.52 \pm 0.02$, with a mass of $0.92 \pm 0.08 M_{\odot}$.

The initial Bayesian evolutionary analysis of WASP-89 (Table 5) gave an age of 12.5 ± 3.1 Gyr, which would likely make it older than the Galactic disk. This raises the possibility that this star is affected by the “radius anomaly” observed in many other late-type stars, particularly those like WASP-89 that show signs of magnetic activity (Hoxie 1973; Popper 1997; López-Morales 2007; Spada et al. 2013). It has been proposed that this is due to the reduction in the efficiency of energy transport by convection, a phenomenon that can be approximated by reducing the mixing length parameter used in the model (Feiden & Chaboyer 2013; Chabrier, Gallardo & Baraffe 2007). The mixing length parameter used to calculate our model grid is $\alpha_{\text{MLT}} = 1.78$. With this value of α_{MLT} GARSTEC reproduces the observed properties of the present day Sun assuming that the composition is that given by Grevesse & Sauval (1998), the overall initial metallicity is $Z = 0.01876$, and the initial helium abundance is

$Y = 0.269$. There is currently no objective way to select the correct value of α_{MLT} for a magnetically active star other than to find the range of this parameter that gives plausible results. Accordingly, we also calculated a Markov chain for the observed parameters of WASP-89 using stellar models with $\alpha_{\text{MLT}} = 1.22$, for which value we find $p(\tau_* < 10 \text{ Gyr}) = 0.91$. By comparing the results for WASP-89 with the two values of α_{MLT} we arrive at a mass of $0.85 \pm 0.05 M_{\odot}$ with the age being indeterminate. This is then compatible with the masses from the spectral analysis and the transit analysis.

8.1. Magnetic activity

WASP-89 shows clear evidence of magnetic activity in the form of a rotational modulation and through star-spots during transit. Three years of WASP-South data all show a ~ 1 per cent modulation at a period near 20 d, and the fourth shows a modulation at half that (10 d), presumably the first harmonic of the rotational period caused by a more complex spot pattern (Table 6, Fig. 7). The average from four different years of WASP-South data is a rotational period of $P_{\text{rot}} = 20.2 \pm 0.4$ d. This, together with our value for the stellar radius, implies a value of $V_{\text{rot}} = 2.2 \pm 0.1 \text{ km s}^{-1}$, which compares to the spectroscopic $V_{\text{rot}} \sin I$ estimate of $2.5 \pm 0.9 \text{ km s}^{-1}$. This is consistent with the WASP-89's spin axis being at 90° to us.

The transit lightcurves from TRAPPIST and EulerCAM show clear star spots, visible as bumps in the transit profile, most clearly at phase 0.997 in the EulerCAM lightcurve from the 02 Oct 2012 (Fig. 4). This raises the issue of whether we are treating the lightcurves correctly in our MCMC

Table 6: Periodogram analysis of the WASP lightcurves for WASP-89. Observing dates are JD – 2450 000, N_{pts} is the number of data points, Amp is the semi-amplitude (in magnitudes) of the best-fit sine wave at the period P found in the periodogram with false-alarm probability FAP.

Year	Dates	N_{pts}	P [d]	Amp	FAP
2008	4622–4752	6648	20.69	0.007	0.006
2009	4970–5116	5589	10.46	0.006	0.072
2011	5691–5858	4072	19.65	0.014	< 0.001
2012	6053–6107	1430	19.57	0.010	0.004

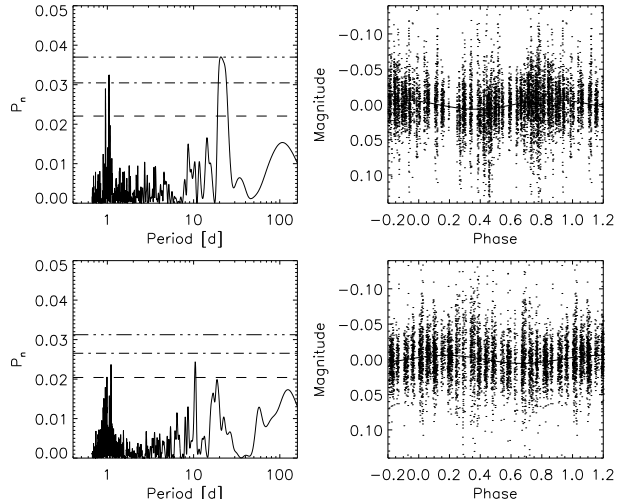


Fig. 7.— Periodograms of the WASP lightcurves for WASP-89 obtained in 2008 (top left) and 2009 (bottom left). Horizontal lines indicate false-alarm probability levels of 0.1, 0.01 and 0.001. Top right shows the 2008 data folded on 20.69 d; bottom right the 2009 data folded in 10.46 d.

analysis (See the discussion in, e.g., Oshagh et al. 2013). When a planet transits a spot we see a slight brightening, and including such data will cause the fitted transit to be shallower. However, any spots that are not transited but still present will do the opposite, causing the transit to be deeper. Thus excluding bumps caused by transited spots would introduce a bias. Without more information on the extent of spottedness there is no secure way of dealing with this. The rotation modulation suggests that the difference between different faces of the star is of order 1 per cent of the brightness, which is comparable to other uncertainties. We have thus chosen to simply combine all the lightcurves in the analysis, effectively averaging over any spots present.

In principle one can use transits of star spots to deduce the orbital alignment (e.g. Tregloan-Reed, Southworth & Tappert 2013). The TRAPPIST and EulerCAM lightcurves from 12 Sep 2012 are of the same transit, as are those from 02 Oct 2012, the latter being 6 orbital cycles (20.1 d) later. There appears to be a spot at phase 0.992 in the 12 Sep lightcurve and a spot at 0.997 in the 02 Oct lightcurve. This could be the same spot being transited one stellar rotation later, which is un-

likely unless the planet’s orbit is aligned with the stellar rotation (or anti-aligned).

If it is the same spot, the difference in the phase of the spot transit implies that the star had rotated by 1.07 cycles (or 0.93 cycles), which translates to a rotation period of 18.8 ± 0.3 d (or 21.7 ± 0.3 d). This is slightly different from the value of 20.2 ± 0.4 d from the WASP data, but the discrepancy might be accounted for by differential rotation.

Thus, we conclude that WASP-89 rotates with a 20-d period and is magnetically active, and that there are indications that the planetary orbit is aligned or anti-aligned. However, we need more extensive star-spot observations and observations of the Rossiter–McLaughlin effect to be sure.

8.2. A massive planet in an eccentric orbit

WASP-89b has a mass of $5.9 \pm 0.4 M_{\text{Jup}}$ and is in a 3.356-d orbit with an eccentricity of 0.19 ± 0.01 . It thus joins a small number of massive planets in short-period, eccentric orbits, of which the most similar are XO-3b ($12 M_{\text{Jup}}$, 3.2 d, $e = 0.26$; Johns-Krull et al. 2008), HAT-P-2b ($8.7 M_{\text{Jup}}$, 5.6 d, $e = 0.52$; Bakos et al. 2007) and HAT-P-21b ($4.0 M_{\text{Jup}}$, 4.1 d, $e = 0.23$; Bakos et al. 2011).

It is worth noting, though, that those three planets orbit stars of spectral type F5, F8 and G3, respectively. WASP-89 is the first known K star hosting a massive planet in a short-period eccentric orbit ($M > 1 M_{\text{Jup}}$; $P < 6$ d; $e > 0.1$). The magnetic activity of WASP-89 could be related to the hosting of a massive, short-period planet, since magnetic activity might be enhanced in hot-Jupiter hosts (e.g. Poppenhaeger & Wolk 2014).

Planets in eccentric, short-period orbits are of particular interest in that their rotation cannot be fully phase-locked to their orbit, and so they must experience large differences in radiative forcing around the orbit. Thus they can tell us about the dynamics of giant-planet atmospheres (e.g. Wong et al. 2014 and references therein).

The usual explanation for the occurrence of such eccentric orbits in short-period hot Jupiters is that they are moved inwards by a process of “high eccentricity migration”, followed by circularisation (e.g. Rasio & Ford 1996; Fabrycky & Tremaine 2007; Naoz et al. 2011; Socrates et al. 2012a).

The circularisation timescale can be estimated from (Adams & Laughlin 2006, eqn 3):

$$\tau_{\text{cir}} \approx 1.6 \text{ Gyr} \times \left(\frac{Q_{\text{P}}}{10^6}\right) \times \left(\frac{M_{\text{P}}}{M_{\text{Jup}}}\right) \times \left(\frac{M_{\star}}{M_{\odot}}\right)^{-3/2} \\ \times \left(\frac{R_{\text{P}}}{R_{\text{Jup}}}\right)^{-5} \times \left(\frac{a}{0.05 \text{ AU}}\right)^{13/2}$$

The value of the quality factor, Q_{P} , is unclear, but if we take it as 10^5 (e.g. Socrates, Katz & Dong 2012b), then we obtain for WASP-89b a circularisation timescale of ~ 2 Gyr. Here, the large mass of the planet prevents circularisation in less than a Gyr despite the short orbit. This timescale is in line with the gyrochronological age of the host star, and thus the fact that the planet has not circularised is consistent. Tidal damping of eccentricity is expected to occur faster than damping of obliquity or inwards orbital decay (Matsumura, Peale & Rasio 2010), and thus we would expect the current values of these properties to be direct products of the high-eccentricity migration.

Acknowledgements

WASP-South is hosted by the South African Astronomical Observatory and we are grateful for their ongoing support and assistance. Funding for WASP comes from consortium universities and from the UK’s Science and Technology Facilities Council. The Euler Swiss telescope is supported by the Swiss National Science Foundation. TRAPPIST is funded by the Belgian Fund for Scientific Research (Fond National de la Recherche Scientifique, FNRS) under the grant FRFC 2.5.594.09.F, with the participation of the Swiss National Science Foundation (SNF). This paper includes observations made with the RISE photometer on the 2.0-m Liverpool Telescope under PATT program PL14A10. The Liverpool Telescope is operated on the island of La Palma by Liverpool John Moores University in the Spanish Observatorio del Roque de los Muchachos of the Instituto de Astrofísica de Canarias with financial support from the UK Science and Technology Facilities Council. M. Gillon and E. Jehin are FNRS Research Associates. A.H.M.J. Triaud is a Swiss National Science Foundation Fellow under grant P300P2-147773. L. Delrez acknowledges the support of the F.R.I.A. fund of the FNRS.

REFERENCES

- Adams, F. C., Laughlin, G., 2006, *ApJ*, 649, 1004
- Anderson D. R. et al., 2012, *MNRAS*, 422, 1988
- Anderson D. R. et al., 2014, *MNRAS*, submitted (arXiv:1410.3449)
- Anderson D. R. et al., 2014, *MNRAS*, 445, 1114
- Asplund, M., Grevesse, N., Sauval, A. J., Scott, P., 2009, *ARA&A*, 47, 481
- Bakos, G. Á. et al., 2007, *ApJ*, 670, 826
- Bakos, G. Á. et al., 2011, *ApJ*, 742, 116
- Barnes, S.A. 2007, *ApJ*, 669, 1167
- Bouchy, F. et al. *A&A*, 519, A98
- Chabrier G., Gallardo J., Baraffe I., 2007, *A&A*, 472, L17
- Claret, A., 2000, *A&A*, 363, 1081
- Collier Cameron, A., et al., 2007a, *MNRAS*, 375, 951
- Collier Cameron, A., et al., 2007b, *MNRAS*, 380, 1230
- Doyle, A.P. et al. 2013, *MNRAS*, 428, 3164
- Doyle, A.P. et al. 2014, *MNRAS*, 444, 3592
- Fabrycky, D., Tremaine, S., 2007, *ApJ*, 669, 1298
- Gray D.F., 2008, *The observation and analysis of stellar photospheres*, 3rd Edition (Cambridge University Press)
- Feiden G. A., Chaboyer B., 2013, *ApJ*, 779, 183
- Grevesse N., Sauval A. J., 1998, *Space Sci. Rev.*, 85, 161
- Hellier, C. et al., 2012, *MNRAS*, 426, 739
- Hellier, C. et al., 2014, *MNRAS*, 440, 1982
- Hoxie D. T., 1973, *A&A*, 26, 437
- Jehin, E. et al., 2011, *Messenger*, 145, 2
- Johns-Krull, C. M., 2008, *ApJ*, 677, 657
- Lendl, M. et al., 2012, *A&A*, 544, A72
- López-Morales M., 2007, *ApJ*, 660, 732
- Matsumura, S., Peale, S. J., Rasio, F. A., 2010, *ApJ*, 725, 1995
- Maxted, P.F.L. et al. 2011, *PASP*, 123, 547
- Maxted, P.F.L., Serenelli, A. M., Southworth, J., 2014, *A&A*, submitted
- Naoz, S., Farr, W. M., Lithwick, Y., Rasio, F. A., Teyssandier, J., 2011, *Nature*, 473, 187
- Oshagh, M., Santos, N. C., Boisse, I., Boué, G., Montalto, M., Dumusque, X., Haghhighipour, N. 2013, *A&A*, 556, A19
- Pollacco, D., et al., 2006, *PASP*, 118, 1407
- Poppenhaeger, K., Wolk, S. J., 2014, *A&A*, 565, L1
- Popper D. M., 1997, *AJ*, 114, 1195
- Rasio, F. A., Ford, E. B., 1996, *Science*, 274, 954
- Serenelli, A. M., Bergemann, M., Ruchti, G., Casagrande, L., 2013, *MNRAS*, 429, 3645
- Sestito, P. & Randich, S., 2005, *A&A*, 442, 615
- Smith A. M. S. et al. 2012, *AJ*, 143, 81
- Socrates, A., Katz, B., Dong, S., Tremaine, S., 2012a, *ApJ*, 750, 106
- Socrates, A., Katz, B., Dong, S., 2012, arXiv:1209.5724
- Southworth J., 2011, *MNRAS*, 417, 2166
- Spada F., Demarque P., Kim Y.-C., Sills A., 2013, *ApJ*, 776, 87
- Steele, I. A., Bates, S. D., Gibson, N., Keenan, F., Meaburn, J., Mottram, C. J., Pollacco, D., Todd, I., 2008, *SPIE*, 70146J
- Tregloan-Reed, J., Southworth, J., Tappert, C., 2013, *MNRAS*, 428, 3671
- Weiss, A., Schlattl, H., 2008, *Ap&SS*, 316, 99
- Wong, I. et al., 2014, *ApJ*, 794, 134
- Zacharias, N., Finch, C. T., Girard, T. M., Henden, A., Bartlett, J. L., Monet, D. G., Zacharias, M. I. 2013, *AJ*, 145, 44

This 2-column preprint was prepared with the AAS L^AT_EX macros v5.2.

Table 7: Radial velocities.

BJD-2400000 (UTC)	RV (km s ⁻¹)	σ_{RV} (km s ⁻¹)	Bisector (km s ⁻¹)
WASP-74:			
55795.60542	-15.8781	0.0045	-0.0067
55796.64971	-15.6394	0.0047	-0.0094
55802.72044	-15.6772	0.0056	0.0026
55820.55636	-15.7453	0.0042	0.0028
55823.52316	-15.8463	0.0060	0.0014
55824.54772	-15.6601	0.0045	-0.0213
55826.57775	-15.6553	0.0049	-0.0019
55827.50202	-15.8600	0.0054	-0.0132
55828.57525	-15.6596	0.0051	-0.0147
55829.63956	-15.8690	0.0044	0.0028
55830.50481	-15.6975	0.0050	-0.0227
55832.53917	-15.7364	0.0042	0.0048
55834.53461	-15.7850	0.0042	-0.0112
55835.53651	-15.7357	0.0050	-0.0019
55851.58947	-15.7856	0.0048	0.0015
56049.91441	-15.9043	0.0041	-0.0147
56103.75557	-15.8386	0.0039	-0.0158
56150.65595	-15.8523	0.0051	-0.0261
56152.55759	-15.8601	0.0052	-0.0277
56212.54690	-15.8647	0.0042	0.0007
WASP-83:			
55626.85323	31.5152	0.0160	-0.0290
55648.77839	31.5828	0.0120	0.0340
55651.73866	31.4915	0.0162	-0.0095
55675.76117	31.5583	0.0176	0.0029
55676.66336	31.5096	0.0132	0.0412
55677.75049	31.5340	0.0123	0.0106
55679.65881	31.5543	0.0109	0.0237
55680.67015	31.5312	0.0148	0.0003
55682.61842	31.5544	0.0081	-0.0127
55683.69704	31.5697	0.0093	0.0069
55684.70318	31.5667	0.0100	0.0015
55707.63183	31.5492	0.0114	0.0389
55711.55909	31.4847	0.0194	0.0092
55721.53003	31.5056	0.0117	-0.0133
55767.53761	31.5751	0.0141	0.0194
55768.48367	31.5820	0.0133	0.0048
55769.49626	31.5754	0.0092	0.0221
55952.79597	31.5772	0.0083	0.0112
55958.80682	31.5390	0.0089	-0.0186
55978.72739	31.5360	0.0131	0.0089
55981.69825	31.5742	0.0148	-0.0285
55982.78430	31.5790	0.0094	-0.0113
55983.85735	31.5348	0.0091	-0.0091
55984.67552	31.5218	0.0097	0.0191
55985.69305	31.5433	0.0097	0.0102
56030.67402	31.5659	0.0136	0.0052
56038.67878	31.5257	0.0149	-0.0179
56336.84838	31.5461	0.0115	0.0185

BJD-2400000 (UTC)	RV (km s ⁻¹)	σ_{RV} (km s ⁻¹)	Bisector (km s ⁻¹)
WASP-89:			
55685.90591	21.8497	0.0245	-0.0109
56123.72535	20.4472	0.0315	-0.0556
56124.69378	20.6905	0.0303	-0.0124
56125.75998	22.0629	0.0296	-0.0349
56126.68173	20.8330	0.0242	0.1185
56136.84966	20.7044	0.0486	0.1745
56150.73985	20.4600	0.0794	0.0443
56151.77120	20.9629	0.0503	0.1013
56154.55728	20.4647	0.0630	0.1552
56158.71898	21.2050	0.0527	0.0643
56159.55775	21.9642	0.0629	0.1241
56159.78044	21.7811	0.0685	0.1462
56181.67023	20.6210	0.0240	-0.0228
56182.64854	21.8869	0.0278	0.0953
56184.60865	20.4188	0.0268	0.0246
56186.53071	21.9080	0.0464	0.0243
56187.54974	20.5000	0.0723	0.0951
56203.56053	21.4453	0.0526	0.0432
56212.57303	21.4703	0.0364	-0.0872
56419.82154	20.5757	0.0407	0.0355

Bisector errors are twice RV errors

Bisector errors are twice RV errors